# Spin-state Equilibria in Non-aqueous Solution and Quantum-mechanical Investigations of Iron(II) and Nickel(II) Complexes with 4-Substituted 2,6-Bis(benzimidazol-2-yl)pyridines†

**Wolfgang Linert,* Michael Konecny and Franz Renz**
*Institute of Inorganic Chemistry, Technical University of Vienna, Getreidemarkt-9/153, A-1060, Vienna, Austria*

Cationic complexes with a series of tridentate ligands, L = 4X-substituted 2,6-bis(benzimidazol-2-yl)-pyridines, $[ML_2][ClO_4]_2$ (M = Fe or Ni; X = H, OH or Cl), were isolated and characterized, together with the free pyridines, by elemental analysis, Fourier-transform IR, $^1H$ NMR and UV/VIS spectroscopy. The syntheses were performed *via* condensation of *o*-phenylenediamine with 4-substituted pyridine-2,6-dicarboxylic acids. Ligand-field parameters were estimated for the nickel complexes. The $[FeL_2]^{2+}$ species show thermally induced spin-crossover behaviour ($^1A_1 \longrightarrow {}^5T_{2g}$) which has been investigated in methanol, nitromethane and 20% (v/v) dimethylformamide in MeOH. The behaviour is complicated by two complex dissociation equilibria, for which equilibrium constants have been evaluated. Ligand substitution is reflected in a change of the spin state in solution [$\mu_{eff}$ = 2.50, X = H; 4.19, OH; and 4.49 $\mu_B$, Cl at 295 K, in MeOH) and in the metal-to-ligand charge-transfer band (500–557 nm); when M = Fe and X = H there is a pronounced spin-crossover equilibrium in methanolic solution ($\mu_{eff}$ = 1.31–3.45 $\mu_B$ for 213–328 K). A small variation of the magnetic moments when M = Fe and X = OH ($\mu_{eff}$ = 3.77–4.73 $\mu_B$ at 220–332 K) might indicate a temperature-variable population of the $^5E_g$ sublevel or variation in hydrogen bonding. The results are compared with quasi-relativistic quantum-mechanical calculations, and the spin-crossover behaviour of the new ligands, L, with substituents X = CHO, $NH_2$, CN, Me, $NO_2$, OH, $CONH_2$, COCl, SH, F, Cl, Br or I has been estimated. The differences in the calculated heats of formation between the high-and low-spin forms of $[FeL_2]^{2+}$ when plotted against Δδ (=$^1H$ NMR *para* increment for substituents X in benzene) show a turning point in the region around X = H and in this region spin-crossover behaviour is observed. Outside this region there is very little or no such behaviour and it is therefore possible to predict the spin-crossover behaviour for other substituents X from the Δδ value.

Thermochromism due to thermally induced equilibria between low- (l.s.) and high-spin (h.s.) states of iron(II) complexes can be observed when the potential minima of the $^1A_1$ and the $^5T_2$ surfaces are so similar in energy that both can be thermally populated.[1] The ligand-field splitting might then be overcome by the spin-pairing energy. Such spin-crossover phenomena have been investigated in the solid state,[2–4] and in solution,[5–12] where, however, solvolysis,[6,7,11] ligand- and anion-exchange reactions,[7] complex deprotonation[10] and hydrogen-bonding[5] complicate the situation. Previous studies on bis[2,6-bis(benzimidazol-2-yl)pyridine]iron(II) perchlorate have shown[10,11] that this complex is a promising candidate for further investigations of spin-crossover phenomena in solution. In the present work we have studied the effect of varying the substituent X in the 4 position in the pyridine ring of the ligand L. The 4-position was chosen because any influence on the spin equilibrium would be due to electronic effects alone, with no direct steric influence.

A generalized reaction scheme to describe the complex-formation equilibria and the thermochromic behaviour of these complexes is given in Scheme 1 [solv = solvent, L = 4-substituted 2,6-bis(benzimidazol-2-yl)pyridine]. It shows that mono and bis complexes are formed in consecutive steps and that a spin-crossover equilibrium of the bis complexes occurs. This scheme is simpler than the mechanism proposed earlier[10,11] as the present results suggest that in MeOH solution $FeL_3$ (with L acting as a bidentate ligand) is formed

$$[Fe(solv)_6]^{2+} + 2L \underset{-3solv}{\overset{K_1}{\rightleftharpoons}} [Fe(solv)_3L]^{2+} + L \underset{-3solv}{\overset{K_2}{\rightleftharpoons}} [FeL_2]^{2+}\ (l.s.)$$

$$K_{sc} \Big\updownarrow$$

$$[FeL_2]^{2+}\ (h.s.)$$

**Scheme 1**

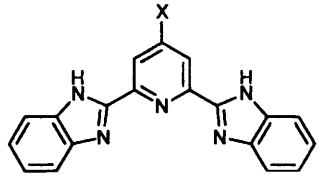

L

in only negligible concentrations. From the observed thermochromism of the complex in solution and its magnetic properties the equilibrium constants ($K_1$ and $K_2$), the spin-equilibrium constants ($K_{sc}$) and the associated thermodynamic parameters ($\Delta H_{sc}$, $\Delta S_{sc}$) of the spin-state equilibria between the l.s. and h.s. states were evaluated.

## Methods

*Solvents.*—The water content of all solvents except acetone was below 100 mg $dm^{-3}$ (Karl–Fischer titration). Commercial grade methanol was refluxed over CaO for 24 h and fractionally

† *Non-SI units employed:* $\mu_B \approx 9.274 \times 10^{-24}$ J $T^{-1}$, bar = $10^5$ Pa, eV ≈ $1.60 \times 10^{-19}$ J.

distilled. Acetone was twice distilled after refluxing over $CaSO_4$. Acetonitrile was refluxed once off NaOH and twice off $P_2O_5$. Propylene carbonate (pyc, 4-methyl-2-oxo-1,3-dioxolane) was refluxed for 24 h under reduced pressure and subsequently fractionally distilled. Nitromethane [Fa. Riedel, 99% (GC)] and dimethylformamide (dmf) were used as received.

*Ligands and Complexes.—Starting materials.* The compounds $FeCl_2 \cdot 4H_2O$ (Aldrich), $Ni(ClO_4)_2 \cdot 6H_2O$ (Merck) and $NaClO_4 \cdot H_2O$ (Fluka), analytical grade, were used as received. 4-Hydroxypyridine-2,6-dicarboxylic acid was prepared from acetone and ethyl oxalate[13] *via* chelidonic acid (4-oxo-4*H*-pyran-2,6-dicarboxylic acid).[14] 4-Chloropyridine-2,6-dicarboxylic acid was synthesised from 4-hydroxypyridine-2,6-dicarboxylic acid and $PCl_5$.[15] 2,6-Bis(benzimidazol-2-yl)pyridine was prepared by the method of Addison and Burke[10,11,16] and recrystallized three times from methanol.

2,6-*Bis*(*benzimidazol-2-yl*)-4-*hydroxypyridine*. 4-Hydroxypyridine-2,6-dicarboxylic acid[14] (14.66 g, 80 mmol) and *o*-phenylenediamine (19.04 g, 172 mmol) were suspended in phosphoric acid (85%, 160 $cm^3$) and kept, with vigorous stirring, at 210–220 °C for 6 h. After cooling, the resulting blue melt was poured into cold water (3 $dm^3$), and the precipitate was filtered off and added to hot 10% aqueous sodium carbonate solution (1 $dm^3$). The resulting solid was filtered off and dried at 20 mbar and 100 °C. The product was dissolved in hot methanol (30 $cm^3$) saturated with sodium carbonate, diluted with water to 300 $cm^3$ and acidified with 15% hydrochloric acid to pH 1. The white product was filtered off and extracted several times with boiling methanol (1 $dm^3$). The collected extracts were evaporated until precipitation began (*ca.* 500 $cm^3$). Cooling overnight yielded colourless crystals which were filtered off, washed with methanol and diethyl ether, dried at 20 mbar and 120 °C, yield 17.1 g (65%), m.p. > 250 °C (Found: C, 64.9; H, 4.55; N, 19.7. Calc. for $C_{19}H_{13}N_5O \cdot 1.5H_2O$: C, 64.4; H, 4.35; N, 19.8%). $^1H$ NMR ($C_2D_5OD$): δ 7.36 (s, pyridine ring), 7.30–7.15, 6.86–6.82 (m, benzene ring).

2,6-*Bis*(*benzimidazol-2-yl*)-4-*chloropyridine* was prepared analogously. Yield 18.5 g (67%), m.p. > 250 °C (Found: C, 60.4; H, 4.05; Cl, 8.65; N, 18.0. Calc. for $C_{19}H_{12}ClN_5 \cdot 2H_2O$: C, 59.8; H, 3.95; Cl, 9.25; N, 18.3%). $^1H$ NMR ($D_2O$–NaOD): δ 7.11 (s, pyridine ring), 7.45–7.37, 6.98–6.89 (m, benzene ring).

$[NiL_2][ClO_4]_2$. A hot solution of the respective free pyridine L (4 mmol $dm^{-3}$) in methanol (1 $dm^3$) was combined with a saturated solution of 2 mmol $dm^{-3}$ $Ni(ClO_4)_2 \cdot 6H_2O$ in methanol yielding a deep blue solution. The solution was evaporated at 20 mbar to about 200 $cm^3$ and the same volume of diethyl ether added. The mixture was cooled overnight to give a light green or lilac solid which was filtered off, washed twice with cooled methanol (10 $cm^3$) and diethyl ether (10 $cm^3$), dried in air and stored over $CaCl_2$ under reduced pressure (yield between 93 and 95%): X = H, light green (Found: C, 50.7; H, 2.90; Cl, 8.01; N, 15.6. Calc. for $C_{38}H_{27}Cl_2N_{10}NiO_8$: C, 51.9; H, 3.00; Cl, 8.05; N, 15.9%); X = OH, lilac (Found: C, 46.5; H, 3.10; N, 13.8. Calc. for $C_{38}H_{26}Cl_2N_{10}NiO_{10} \cdot 4H_2O$: C, 46.4; H, 3.50; N, 14.2%); X = Cl, lilac (Found: C, 47.9; H, 3.35; N, 14.1. Calc. for $C_{38}H_{26}Cl_4N_{10}NiO_8 \cdot 0.5H_2O$: C, 47.4; H, 2.65; N, 14.6%).

$[FeL_2][ClO_4]_2$. A hot oxygen-free solution of free pyridine L (6 mmol) in methanol (1 $dm^3$) was combined with a saturated solution (20 $cm^3$) of $FeCl_2 \cdot 4H_2O$ (3 mmol) in methanol to give a deep red solution.[7] This was evaporated at 20 mbar to about 150 $cm^3$. Solid $NaClO_4 \cdot H_2O$ (12 mmol) was added and the solution cooled overnight. The resulting magenta crystals were filtered off, washed twice with cooled methanol (10 $cm^3$) and diethyl ether (20 $cm^3$), dried at 20 mbar and stored over $CaCl_2$ under reduced pressure (yield 92–95%); X = H (Found: C, 51.9; H, 2.95; N, 15.9. Calc. for $C_{38}H_{26}Cl_2FeN_{10}O_8$: C, 52.0; H, 3.00; N, 15.9%); X = OH (Found: C, 47.2; H, 3.10; N, 14.3. Calc. for $C_{38}H_{26}Cl_2FeN_{10}O_{10} \cdot 3H_2O$: C, 47.4; H, 3.35; N, 14.5%); X = Cl (Found: C, 45.4; H, 2.90; N, 13.6. Calc. for $C_{38}H_{24}Cl_4FeN_{10}O_8 \cdot 3.5H_2O$: C, 45.2; H, 3.00; N, 13.9%).

All complexes were prepared in a nitrogen atmosphere with solvents deoxygenated by nitrogen gas.

*Solutions.*—Spectrophotometric titrations using ligand solutions were performed over a concentration range of $1 \times 10^{-4}$–$5 \times 10^{-4}$ mol $dm^{-3}$ $Fe^{2+}$ with a $L:Fe^{2+}$ ratio between 0 and 20:1 when X = H and with $8 \times 10^{-5}$–$2 \times 10^{-4}$ mol $dm^{-3}$ $Fe^{2+}$ with a $L:Fe^{2+}$ ratio between 0 and 15:1 for the X = Cl and X = OH species. The solubilities of L when X = Cl or OH are lower than that when X = H in methanol. Spectroscopic and magnetic properties were investigated with complex concentrations of $2 \times 10^{-4}$–$5 \times 10^{-4}$ mol $dm^{-3}$ using an excess of ligand (saturated ligand solution in the case of nitromethane) to avoid ligand dissociation at higher temperatures. All solutions were prepared by using deoxygenated solvents and a Schlenk-type technique under a nitrogen atmosphere in a glove-box to avoid oxidation of the complex.

*Spectrophotometric Measurements.*—The UV/VIS spectra were run on a Hitachi U-2000 spectrophotometer equipped with an electronic thermostatted cell holder (Hitachi) for the range 0–100 (± 0.5) °C. The temperature was recorded with a copper–constantan thermocouple in the cell. A homogeneous temperature distribution within the cells was ensured by using a magnetic stirrer. Below room temperature (≤ 20 °C) dry nitrogen gas was blown into the cell compartment. Owing to the thermochromism of the system under study, temperature constancy could easily be observed on an absorbance *vs.* time plot; a constant value was reached after 6 min. Molar absorption coefficients, $\varepsilon_{obs}$, were corrected for changes in solvent density arising from the temperature variation.[13,14] Far-IR measurements were made with a Nicolet 20F far-IR vacuum spectrometer (FTIR) with a triglycine sulfate (room temperature) detector using polyethylene wafers. The data collection was accomplished with the Happ–Genzel apodization function.

*Magnetic Measurements.*—Proton NMR spectra were run on a Bruker AC 250 FT spectrometer operating at 250 MHz. High-precision NMR sample tubes of type 528-PP (Wilmad Glass Co.) with sealed Wilmad coaxial inserts (WGS-5BL) containing 5% $SiMe_4$ in $(CD_3)_2CO$ were used as external standard and as instrument lock. Magnetic susceptibilities in solution were measured by the Evans $^1H$ NMR method[17] using the solvent methanol for temperature calibration.[18] The results were corrected for changes in solvent density with temperature.[19,20] 0.5% (v/v) Dioxane was used as internal reference.

*Quantum-mechanical Calculations.*—Quantum-chemical calculations were performed on an IBM-ES/9021-720 computer using a quasi-relativistic (QR-) intermediate neglect of differential overlap (INDO) program.[21] This program includes a non-empirical version of the CNDO/1 method and dominant relativistic effects[22,23] as well as one-electron corrections.[24] It is set up for calculations on systems containing even heavy transition-metal ions,[25] including variations due to the spin-state of the system, and considers solvation and substituent effects.[26] Geometries were based on X-ray diffraction data.[27] When no complete set of coordinates was available, energy-minimization procedures were used to obtain optimum geometries.

## Results and Discussion

Far-IR absorption maxima of the compounds are given in Table 1. Assignments are based on earlier investigations of unsubstituted bbzmpy or various metal complexes of it.[19] The in-plane vibration of the pyridine ring is almost unchanged by co-ordination whereas the out-of-plane vibration is shifted to

higher wavenumbers. Ligand vibrations involving N atoms are significantly shifted to lower wavenumbers due to co-ordination.

*UV/VIS Spectra.*—Table 2 gives the d–d transition absorption maxima of the $[NiL_2][ClO_4]_2$ complexes. They are assigned to the transitions: $\nu'$, $^3A_{2g}(F) \longrightarrow {}^1E_g(D)$; $\nu_2$, $^3A_{2g}(F) \longrightarrow {}^3T_{1g}(F)$; and $\nu_1$, $^3A_{2g}(F) \longrightarrow {}^3T_{2g}(F)$. The transition $\nu_1$ in octahedral nickel(II) complexes is directly related to the crystal-field splitting $10Dq$ ($=\Delta_o$). A shoulder at $\nu'$ shows a spin-forbidden transition, which can be observed for most octahedral nickel(II) complexes with α-diimine ligands.[14,18,20] The $^3A_{2g} \longrightarrow {}^3T_{2g}$ and $^3A_{2g} \longrightarrow {}^1E_g$ transitions yield, *via* spin–orbit coupling, a mixture of both $^1E_g$ and $^3T_{2g}$ stimulated states.[14] From the empirical relations (1) and (2) it is possible to calculate the position of pure $\nu_1$ and $\nu'$

$$\nu'(^3A_{2g} \longrightarrow {}^1E_g) = 13\,100 - 1100\,(\varepsilon_1/\varepsilon') \quad (1)$$

$$\nu_1 = 10Dq\,(^3A_{2g} \longrightarrow {}^3T_{2g}) = 12\,000 + 1370\,[(\varepsilon_1/\varepsilon') - 1] \quad (2)$$

transitions from the spectra. Here $\varepsilon_1$, $\varepsilon'$ are the molar absorption coefficients of the band associated with the higher and the lower energies in the 12 000 $cm^{-1}$ region (Table 3). Spin crossover of iron(II) complexes can be expected when the corresponding complex of $Ni^{II}$ has a $10Dq$ value between 11 300 and 11 900 $cm^{-1}$. The pronounced differences between solid-state and solution $10Dq$ values underlines that it is hardly possible to predict spin-crossover behaviour in solution based on available solid-state data. This difference is larger for the Cl- and OH-substituted species and might suggest that in the solid state the respective complexes of $Fe^{2+}$ occur in their low-spin state whereas in solution the high-spin state should be preferred. However, the observations indicate the high-spin state at room temperature for all complexes. The value of $10Dq$ increases in the solid state and decreases in MeOH solution with temperature.

Temperature-dependent UV/VIS spectra of the $[FeL_2]^{2+}$ complexes dissolved in methanol with excess of ligand (to reduce ligand dissociation) are given in Table 4 and in Figs. 1–3. Absorption maxima are found at 557 nm for X = H, at 520 nm for X = OH and at 502 nm for X = Cl in MeOH. Absorption maxima for X = H are found at 554 nm in nitromethane and at 559 nm in 20% (v/v) dmf–MeOH. These bands can be assigned[28,29] as charge transfer (c.t.) from a filled metal d orbital to an empty ligand π* orbital. Between 600 and 800 nm d–d absorption bands are found.[7,8] With ligand substitution from X = H to OH and Cl the colour of the solution changes at

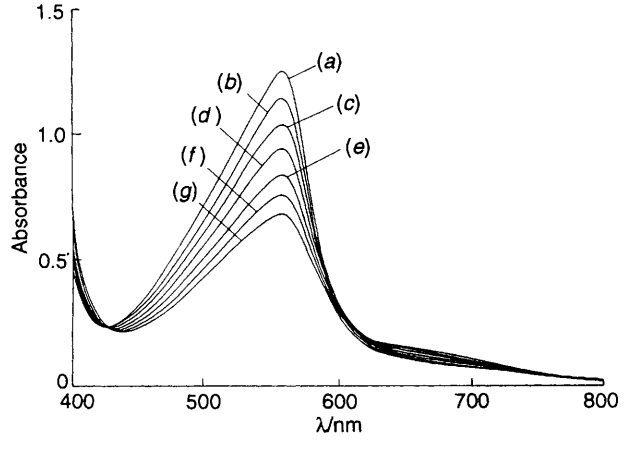


**Fig. 1** The UV/VIS absorption spectra of $[FeL_2][ClO_4]_2$ where X = H with an excess of ligand at different temperatures in methanol: 1.453 × $10^{-4}$ mol $dm^{-3}$ $[FeL_2]$, L:$Fe^{2+}$ = 20:1 and $T$ = (*a*) 276, (*b*) 285, (*c*) 294, (*d*) 303, (*e*) 314, (*f*) 322 and (*g*) 331 K

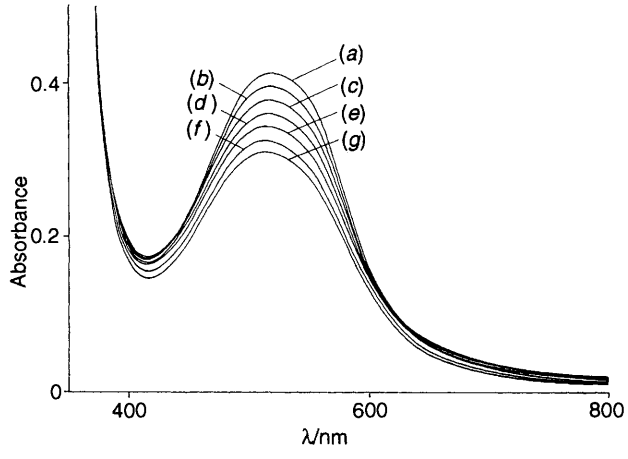


**Fig. 2** The UV/VIS absorption spectra of $[FeL_2][ClO_4]_2$ where X = OH with an excess of ligand at different temperatures in methanol: 2.234 × $10^{-4}$ mol $dm^{-3}$ $[FeL_2]$, L:$Fe^{2+}$ = 8.67:1 and $T$ = (*a*) 277, (*b*) 285, (*c*) 294, (*d*) 303, (*e*) 312, (*f*) 322 and (*g*) 331 K

**Table 1** Wavenumbers ($cm^{-1}$) and assignments in the far-IR spectra of $[ML_2][ClO_4]_2$ at room temperature

| X = OH | M = Ni | Fe | X = Cl | M = Ni | Fe | Assignment |
|---|---|---|---|---|---|---|
| 622m | 662s | 623s | 621s | 621s | 621s | δ(pyridine) in plane |
| 606s | 595w | | 606s | | | Ligand-ring vibration |
| 587m | | 584m | | | 584m | |
| 573m | 572m | 570s | 573m | 571m | 571m | Ligand-ring vibration |
| 567m | | | | | | |
| 558s | | | 558m | 558m | | |
| 542s | 541m | 541m | 542s | 541s | 541s | Ligand-ring vibration |
| | | | 504s | 500m | 500m | ClC ring vibration |
| | 471m | 474m | | 470m | 471m | Metal-ligand combination |
| 461w | | | | 458w | | ν(Ni–N) |
| 439s | 435s | 436s | 439s | 435s | 435s | N-ring vibration |
| | 404s | | | 405w | | ν(Fe–N) (h.s. state) |
| 368s | 387w | 387s | 368w | 387w | 387w | δ(pyridine) out of plane |
| 353w | 353w | | | | | |
| 341m | | | 341m | 339w | 340m | |
| 309s | | | | 310s | 294s | |
| 281s | | 283w | | 281s | 280w | |
| 269m | | | | 269m | 267m | |
| 255m | | | | | | |
| 241s | 241m | | 236s | 241m | 240w | |

**Table 2** Spectral parameters of $[NiL_2][ClO_4]_2$ complexes

| X | $\lambda_1$/nm | $\lambda'$/nm | $\lambda_2$/nm |
|---|---|---|---|
| H[a] | 861 | 780 | 562 |
| H[b] | 829 | 780 | 543 |
| Cl[a] | 810 | 773 | — |
| Cl[b] | 866 | 773 | 554[c] |
| OH[a] | 809 | 776 | 534 |
| OH[b] | 866 | 776 | 564 |

[a] Solid state. [b] In MeOH solution. [c] Shoulder at 623 nm.

**Table 3** Ligand-field parameters and corrected energies of $\nu'$ [*i.e.* $^3A_{2g}(F) \longrightarrow {}^1E_g(D)$] for $[NiL_2][ClO_4]_2$ complexes

| X | $\varepsilon_1/\varepsilon'$ | $10Dq_{corr}$[a]/cm$^{-1}$ | $\nu'_{corr}$[a]/cm$^{-1}$ |
|---|---|---|---|
| H[b] | 0.88 | 11 840 | 12 130 |
| H[c] | 0.72 | 11 620 | 12 310 |
| Cl[b] | 0.95 | 11 930 | 12 060 |
| Cl[c] | 0.63 | 11 500 | 12 410 |
| OH[b] | 0.96 | 11 950 | 12 040 |
| OH[c] | 0.63 | 11 500 | 12 410 |

[a] According to equations (1) and (2). [b] Solid state. [c] In MeOH solution.

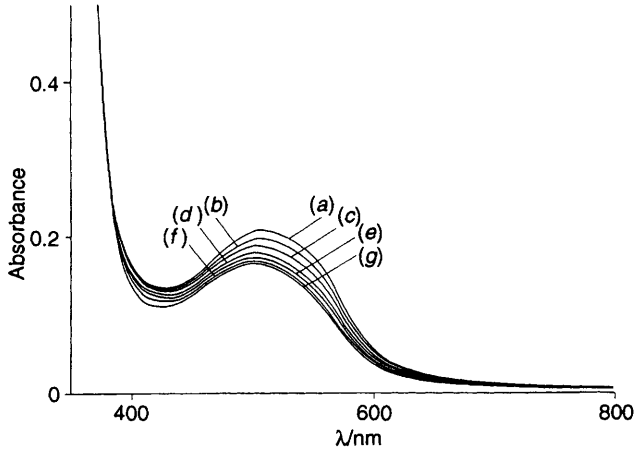


**Fig. 3** The UV/VIS absorption spectra of $[FeL_2][ClO_4]_2$, where X = Cl with an excess of ligand at different temperatures in methanol: $2.112 \times 10^{-4}$ mol dm$^{-3}$ $[FeL_2]$, L:$Fe^{2+}$ = 6.90:1 and $T$ = (*a*) 276, (*b*) 284, (*c*) 293, (*d*) 303, (*e*) 312, (*f*) 322 and (*g*) 331 K

room temperature from red-violet to bluish violet and, finally, to light brown. The c.t. band shifts towards shorter wavelength whereas the d–d transition band shifts to longer wavelength and the molar absorption coefficients gradually become smaller (to almost a quarter of the value for X = H). The energy of the lowest unfilled $\pi$ orbital of the ligand is increased leading to relatively higher energies of the c.t. band whereas the ligand-field splitting is decreased[8] (*i.e.* a hyperconjugative effect arises due to the substituent). This results in an almost pure h.s. state at room temperature for the Cl- and OH-substituted species. The lowering of symmetry from $O_h$ to $D_{2d}$ causes a splitting of the degenerate $t_{2g}$ level into a single and a doubly degenerate level ($b_2$ + e). It is assumed that this splitting $d_\pi(b_2) \longrightarrow \pi_1^*$ and $d_\pi(e) \longrightarrow \pi_1^*$ is responsible for the broader peaks[9,29–31] found for the Cl- and OH-substituted species compared with the unsubstituted complex.

*Complex-formation Equilibria.*—At high ligand to metal ion ratios (L:Fe $\geqslant$ 2.0–20:1) in MeOH the UV/VIS spectrum of the $[FeL_2]^{2+}$ species is found for all ligands. At L:Fe $\leqslant$ 0.5:1 a peak at shorter wavelength, associated with an $[FeL]^{2+}$ species, becomes increasingly important. Fitting of the respective spectrophotometric titration curves for X = H, OH or Cl (Fig. 4) confirms that only two species, $[FeL]^{2+}$ and $[FeL_2]^{2+}$, are formed. Absorption maxima corresponding to the $[FeL]^{2+}$ species are found for X = H at 504 nm, for X = OH at 445 nm, and for X = Cl at 440 nm.

**Table 4** The UV/VIS spectral data for $[FeL_2][ClO_4]_2$, with an without excess of ligand, in non-aqueous solutions

| Solvent | L:$Fe^{2+}$ | Colour | $\lambda_{max}$/nm | $\varepsilon_{max}$/dm$^3$ mol$^{-1}$ cm$^{-1}$ |
|---|---|---|---|---|
| (*a*) X = H[a] | | | | |
| MeOH | 28.0:1 | Red-violet | 557 | 7000 ± 20 |
| MeOH | 2.0:1 | Red-violet | 557 | 4330 ± 20 |
| $Me_2CO$ | 24.0:1 | Red | 555 | 5940 ± 20 |
| $Me_2CO$ | 2.0:1 | Red | 555 | 5560 ± 20 |
| MeCN | 5.7:1 | Red | 552 | 4970 ± 20 |
| MeCN | 2.0:1 | Red | 552 | 4550 ± 20 |
| $MeNO_2$ | Saturated | Light pink | 554 | 6320 ± 20 |
| $MeNO_2$ | 2.0:1 | Light pink | 554 | 5080 ± 20 |
| pyc | 40.0:1 | Red-violet | 555 | 5930 ± 20 |
| pyc | 2.0:1 | Red-violet | 555 | 5180 ± 20 |
| pyc–MeOH[b] | 30.0:1 | Red-violet | 556 | 5650 ± 20 |
| pyc–MeOH[b] | 2.0:1 | Red-violet | 556 | 4880 ± 20 |
| dmf–MeOH[c] | 2.0:1 | Red-violet | 559 | 5200 ± 20 |
| (*b*) X = OH[d] | | | | |
| MeOH | 8.7:1 | Red-violet | 520 | 1800 ± 20 |
| MeOH | 2.0:1 | Light red | 503 | 1440 ± 20 |
| $Me_2CO$ | 2.0:1 | Wine-red | 502 | 1490 ± 20 |
| MeCN | 2.0:1 | Light pink | 498 | 1700 ± 20 |
| $MeNO_2$ | 2.0:1 | Pink | 503 | 2270 ± 20 |
| pyc | 2.0:1 | Wine-red | 501 | 1580 ± 20 |
| dmf | 2.0:1 | Blue | 585 | 3300 ± 50 |
| dmf–MeOH[c] | 5.8:1 | Bluish red | 541 | 2160 ± 20 |
| (*c*) X = Cl[d] | | | | |
| MeOH | 6.9:1 | Wine-red | 502 | 980 ± 20 |
| MeOH | 2.0:1 | Light red | 487 | 620 ± 20 |
| $Me_2CO$ | 2.0:1 | Light red | 490 | 750 ± 20 |
| MeCN | 2.0:1 | Light pink | 487 | 1820 ± 20 |
| $MeNO_2$ | 2.0:1 | Pink | 500 | 2250 ± 20 |
| pyc | 2.0:1 | Light pink | 493 | 1320 ± 20 |
| dmf | 2.0:1 | Light yellow | — | — |
| dmf–MeOH[c] | 5.3:1 | Light red | 490 | 850 ± 20 |

[a] $T$ = 294 K. [b] 50% (v/v) pyc–MeOH. [c] 20% (v/v) dmf–MeOH. [d] $T$ = 298 K.

The large log $K_1$ and log $K_2$ values (Table 5) in relation to comparable ligands [2-(2-pyridyl)imidazole (pyim) and 2,2′-bipyridine (bipy)][32,33] confirm that L (X = H) is acting as a tridentate ligand in both $[FeL]^{2+}$ and $[FeL_2]^{2+}$. Unlike the spin-crossover behaviour of the complexes, the formation constants are, as expected, little influenced by the electron-withdrawing substituents on the ligand.

*Thermally Induced Spin-crossover Behaviour.*—The spin-crossover equilibrium of the $[FeL_2]^{2+}$ complex is reflected in the UV/VIS spectrum by a variation of the intense charge-transfer band in the temperature range 276–331 K (Figs. 1–3). With increasing temperature, the molar absorption coefficient decreases as the high-spin state is increasingly populated.[5,7,9–12] The shape of the d–d bands when X = H at high temperature is almost identical to that found for both X = OH and Cl and these complexes are in their high-spin state at all temperatures.

A value of the molar absorption coefficient of the pure high-spin component ($\varepsilon_{hs}$ = 750 dm$^3$ mol$^{-1}$ cm$^{-1}$) can be estimated from the high-temperature spectrum when X = Cl. Owing to the experimentally limited temperature range, the value of the pure low-spin isomer ($\varepsilon_{ls}$) is not directly accessible and was therefore estimated by means of a least-squares fitting procedure ($\varepsilon_{ls}$ = 13 000 ± 500 dm$^3$ mol$^{-1}$ cm$^{-1}$). Both values agree with literature values.[1,10,11]

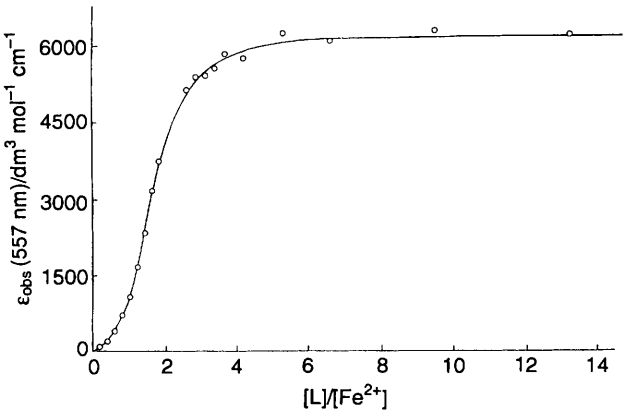


**Fig. 4** Formation curve of $[FeL_2]^{2+}$, where X = H, in methanol at $\lambda_{max}$ = 557 nm and 293 K

**Table 5** Formation constants, absorption maxima of $[FeL_2]^{2+}$, and molar absorption coefficients of $[FeL]^{2+}$ and $[FeL_2]^{2+}$ in methanol at 293 K

| | | $\varepsilon_{max}$/dm$^3$ mol$^{-1}$ cm$^{-1}$ | | | |
|---|---|---|---|---|---|
| X | $\lambda_{max}$/nm | $[FeL]^{2+}$ | $[FeL_2]^{2+}$ | log $K_1$ | log $K_2$ |
| H | 557 | 350 ± 20 | 6600 ± 50 | 5.72 ± 0.05 | 4.35 ± 0.05 |
| OH | 515 | 150 ± 20 | 1800 ± 20 | 5.70 ± 0.05 | 4.44 ± 0.05 |
| Cl | 500 | 150 ± 20 | 1550 ± 20 | 5.67 ± 0.05 | 4.38 ± 0.05 |

However, for a detailed investigation of the magnetic behaviour, a method is required where magnetic moments can be measured directly over a large temperature range. We used Evans' method based on NMR shifts.[17] Magnetic moments of the dissolved complexes were calculated from equations (3) and (4), where $\Delta\Delta\nu$ (in ppm) is the paramagnetic shift of a

$$\chi_{exptl} = (3\Delta\Delta\nu \cdot 0.001/4\pi c) \quad (3)$$

$$\mu_{exptl} = 2.84(\chi T)^{\frac{1}{2}} \quad (4)$$

reference compound, corrected for the diamagnetic contribution of the ligand and $c$ is the molarity of the paramagnetic ion. The diamagnetic correction for the ligand was determined experimentally in a ligand concentration range, [L], from 0 to $1.4 \times 10^{-3}$ mol dm$^{-3}$ in methanol at 293 K; linear concentration dependences (5)–(7) were found. From these relationships,

$$\Delta\Delta\nu = -4.73 \times 10^{-5} + 0.869[L] \text{ for X = H} \quad (5)$$

$$\Delta\Delta\nu = -2.57 \times 10^{-5} + 1.46[L] \text{ for X = OH} \quad (6)$$

$$\Delta\Delta\nu = -2.26 \times 10^{-5} + 1.42[L] \text{ for X = Cl} \quad (7)$$

molar diamagnetic susceptibilities were calculated yielding $\chi_M = -212 \times 10^{-6}$, $-341 \times 10^{-6}$ and $-334 \times 10^{-6}$ cm$^3$ mol$^{-1}$ for X = H, OH and Cl respectively. These values deviate slightly from those derived from Pascal constants[34,35] but are better suited to these calculations of paramagnetic moments as they are based on the same experimental method.

Magnetic susceptibilities of the iron complexes in solution were measured in the temperature range 213–343 K (Table 6). The non-Curie magnetic behaviour when X = H (see Fig. 5) reflects the spin-transition equilibrium. For this complex the magnetic moments are strongest in MeCN, varying between 0.85 (251.7) and 4.51 $\mu_B$ (340 K) and clearly fall between the

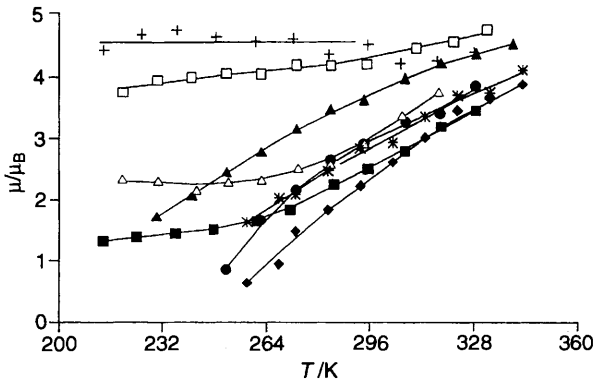


**Fig. 5** Magnetic moments of $[FeL_2][ClO_4]_2$ with an excess of ligand in non-aqueous solution *versus* temperature: X = H in MeOH, $5.580 \times 10^{-4}$ mol dm$^{-3}$ and L:Fe$^{2+}$ = 8.3:1 (△), in $MeNO_2$, $3.437 \times 10^{-4}$ mol dm$^{-3}$ and L:Fe$^{2+}$ = 5.2:1 (*), in $Me_2CO$, $3.0634 \times 10^{-4}$ mol dm$^{-3}$ and L:Fe$^{2+}$ = 7.32:1 (▲), in MeCN, $3.966 \times 10^{-4}$ mol dm$^{-3}$ and L:Fe$^{2+}$ = 7.4:1 (●), in pdc, $5.5525 \times 10^{-4}$ mol dm$^{-3}$ and L:Fe$^{2+}$ = 7.1:1 (◆); X = OH in MeOH, $2.870 \times 10^{-4}$ mol dm$^{-3}$ and L:Fe$^{2+}$ = 5.0:1 (□); X = Cl in MeOH, $2.473 \times 10^{-4}$ mol dm$^{-3}$ and L:Fe$^{2+}$ = 7.3:1 (+)

ranges of those for pure low spin ($S = 0$, *i.e.* 0–0.5 $\mu_B$) and pure high spin ($S = 2$, *i.e.* 5.0–5.5 $\mu_B$) found for similar six-co-ordinated iron(II)–imine complexes.[1,4–8] The temperature dependence is much less pronounced for the Cl- and OH-substituted species. The magnetic moment is *ca.* 4.4 $\mu_B$ for the former and varies between 3.76 and 4.73 $\mu_B$ for the latter, showing that these complexes are permanently in their high-spin state over this temperature range. A possible explanation of the slight temperature dependence when X = OH might be that a temperature-dependent variation of hydrogen bonding between OH groups of the ligand and the MeOH solvent is present. An alternative, but possibly closely related, explanation would be the presence of a variable population of the sublevels of the $^5E_g$ component within the split $^5T_{2g}$ ground state as has been suggested for iron(II) poly(pyrazolyl)borates.[8] Similar magnetic behaviour due to a change of substituent group on the ligand was found for {tris[4-(6*R*-2-pyridyl)-3-azabut-3-enyl]amine}iron(II) complexes[4] (R = H or Me) and for $[Co\{NC_5H_3(CH{=}NR)_2\text{-}2,6\}][PF_6]_2$ complexes[5] (R = Bu$^t$, Pr$^n$, NHMe, $C_6H_4Me$-*p* or $CH_2Ph$).

From the observed magnetic behaviour the spin-crossover equilibrium constant ($K_{sc}$) of $[FeL_2][ClO_4]_2$ when X = H has been evaluated by use of equation (8), where $x$ is the mole

$$K_{sc} = x_{hs}/x_{ls} = (\mu_{exptl}^2 - \mu_{ls}^2)/(\mu_{hs}^2 - \mu_{exptl}^2) \quad (8)$$

fraction of the indicated spin isomer and $\mu_{hs}$ and $\mu_{ls}$ are the effective magnetic moments for the high- and low-spin forms, 5.5 and 0.5 $\mu_B$ respectively. Thermodynamic parameters ($\Delta S_{sc}$ and $\Delta H_{sc}$) were estimated from plots of $\Delta G = -RT \ln K_{sc}$ *vs.* $T$. The $K_{sc}$ values (Table 7) calculated earlier[10,11] from spectrophotometric measurements are significantly larger. We therefore analysed the present data in the same way and also found large values ($\Delta H_{sc}$ = 3.9 kJ mol$^{-1}$, $\Delta S_{sc}$ = 54.21 J K$^{-1}$ mol$^{-1}$, $K_{sc}$ = 0.85). The discrepancy seems to arise from the lack of exact molar absorption coefficients combined with the restricted temperature range available for the spectroscopic measurements. The relatively high $\Delta H_{sc}$ and $\Delta S_{sc}$ values (Table 7) of the complex in 20% (v/v) dmf–MeOH in contrast to those in MeOH may be attributed to solvation of the imidazole proton which might be expected preferentially to stabilize the l.s. form: this effect appears to increase with increasing donor number of the solvent.

*Quasi-relativistic Quantum-mechanical Calculations.*—Calculations have been performed for the $[FeL_2]^{2+}$ complexes

**Table 6** Magnetic moment data for $[FeL_2][ClO_4]_2$ at different temperatures in non-aqueous solvents

| X = H in MeOH | | X = OH in MeOH | | X = Cl in MeOH | | X = H in $Me_2CO$ | |
|---|---|---|---|---|---|---|---|
| $T$/K | $\mu/\mu_B$ | $T$/K | $\mu/\mu_B$ | $T$/K | $\mu/\mu_B$ | $T$/K | $\mu/\mu_B$ |
| 213.7 | 1.31 | 219.8 | 3.76 | 214.0 | 4.41 | 251.7 | 0.85 |
| 223.8 | 1.38 | 230.4 | 3.95 | 225.5 | 4.66 | 262.5 | 1.65 |
| 235.8 | 1.43 | 240.9 | 3.99 | 236.3 | 4.72 | 273.4 | 2.15 |
| 247.7 | 1.50 | 251.7 | 4.05 | 248.5 | 4.62 | 283.8 | 2.65 |
| 261.0 | 1.64 | 262.4 | 4.04 | 260.7 | 4.54 | 294.3 | 2.91 |
| 271.5 | 1.83 | 273.3 | 4.18 | 272.2 | 4.59 | 306.9 | 3.28 |
| 284.8 | 2.24 | 284.0 | 4.17 | 283.3 | 4.34 | 317.9 | 3.40 |
| 295.4 | 2.50 | 295.1 | 4.19 | 295.3 | 4.49 | 328.8 | 3.84 |
| 306.9 | 2.79 | 310.3 | 4.44 | 305.4 | 4.20 | 317.9 | 4.21 |
| 317.9 | 3.19 | 321.7 | 4.54 | 316.7 | 4.24 | 328.8 | 4.35 |
| 328.7 | 3.45 | 332.0 | 4.73 | 328.1 | 4.38 | 340.0 | 4.51 |

| X = H in MeCN | | X = H in pyc | | X = H in $MeNO_2$ | | X = H in 20% (v/v) dmf in MeOH | |
|---|---|---|---|---|---|---|---|
| $T$/K | $\mu/\mu_B$ | $T$/K | $\mu/\mu_B$ | $T$/K | $\mu/\mu_B$ | $T$/K | $\mu/\mu_B$ |
| 230.2 | 1.72 | 230.2 | 0.64 | 258 | 1.62 | 219 | 2.30 |
| 241.1 | 2.06 | 241.1 | 0.94 | 268 | 2.02 | 230 | 2.33 |
| 251.7 | 2.45 | 251.7 | 1.47 | 273 | 2.08 | 241 | 2.13 |
| 262.5 | 2.78 | 262.5 | 1.83 | 283 | 2.47 | 252 | 2.26 |
| 273.3 | 3.16 | 273.3 | 2.22 | 293 | 2.84 | 263 | 2.27 |
| 283.8 | 3.48 | 283.8 | 2.61 | 303 | 2.93 | 273 | 2.48 |
| 294.2 | 3.63 | 294.3 | 3.01 | 313 | 3.36 | 284 | 2.57 |
| 306.9 | 3.98 | 306.9 | 3.46 | 323 | 3.70 | 294 | 2.89 |
| 317.8 | 3.65 | | | 333 | 3.75 | 306 | 3.33 |
| 328.7 | 3.88 | | | 343 | 4.10 | 317 | 3.80 |

**Table 7** Spin-equilibrium constants and thermodynamic parameters of some iron(II)–imine complexes in different solvents from magnetic measurements at 293 K

| Complex | Solvent | $\Delta H$/kJ mol$^{-1}$ | $\Delta S$/J K$^{-1}$ mol$^{-1}$ | $K_{sc}T$ | Ref. |
|---|---|---|---|---|---|
| $[FeL_2][ClO_4]_2$[a] | MeOH | 20.51 ± 0.4 | 58.60 ± 0.4 | 0.26 | This work |
| | dmf (20%)–MeOH | 29.43 ± 0.4 | 93.06 ± 0.4 | 0.38 | This work |
| | $MeNO_2$ | 20.39 ± 0.4 | 60.82 ± 0.4 | 0.36 | This work |
| | $Me_2CO$ | 22.52 ± 0.4 | 68.06 ± 0.4 | 0.39 | This work |
| | MeCN | 17.37 ± 0.4 | 57.26 ± 0.4 | 0.77 | This work |
| | pyc | 23.90 ± 0.4 | 73.88 ± 0.4 | 0.43 | This work |
| | MeOH[b] | 16.53 ± 1.6 | 54.21 ± 2.0 | 0.85 | This work |
| | dmf[b] | 0.925 ± 0.4 | 141.1 ± 1.6 | 0.57 | 6 |
| $[Fe(pybim)_3]BPh_4$[c] | $Me_2CO$ | 19.67 ± 0.4 | 77.86 ± 2.0 | 3.62 | 4 |
| | MeCN (20%)–MeOH | 21.35 ± 1.6 | 92.09 ± 6.8 | 10.00 | 4 |

[a] X = H. [b] From spectroscopic measurements at $\lambda_{max}$ = 557 nm. [c] pybim = 2-(2-pyridyl)benzimidazole.

with X = CHO, $NH_2$, CN, Me, $NO_2$, OH, $CONH_2$, COCl, SH, F, Cl, Br or I. This is a $d^6$ electronic system and has a spin multiplicity of one for the low-spin complex; the four unpaired electrons are assigned a spin multiplicity of five for the high-spin complexes. As starting geometry we used the crystal structure[27] of $[FeL_2]^{2+}$ with X = H and standard values[36,37] of the bond angles and lengths for the substituents X listed. After optimization of the geometry, deviations of *ca.* 2–3% for bond angles and 5–8% for bond distances were found when compared with the crystallographic data, but this is due to the fact that the calculation was performed for molecules in the gas phase (Scheme 2 and Table 8). The calculated bond angles and distances then yield the respective minima for the total energy of the l.s. and h.s. states.

The QR-INDO calculations with different substituents X in $[FeL_2]^{2+}$ (Table 9) were carried out to obtain (*i*) the bond order (Wiberg indices) between the iron and the averaged values of the N-donor atoms of the two substituted pyridine rings (*i.e.* Fe–2N$^1$), (*ii*) the bond order between the iron and the averaged values of the N-donor atoms of the four substituted benzimidazole rings (*i.e.* Fe–4N$^2$), (*iii*) the partial charges on the Fe, two N$^1$ and four N$^2$ atoms, and (*iv*) the difference in the heat of formation between the l.s. (spin multiplicity $m$ = 1) and h.s. complexes ($m$ = 5), *i.e.* $\Delta H_{ls-hs}$. From Table 9 it can be seen that the imidazole nitrogens are bonded more strongly to the iron than are the pyridine nitrogens and the change in the bond order between the h.s. and l.s. in Fe–2N$^1$ is about 0.03 higher than in Fe–4N$^2$. These results can be explained as a steric effect because the pyridine nitrogen, N$^1$, is much less geometrically flexible than is the imidazole nitrogen, N$^2$. In the case of a change in the electronic structure around the iron, such as is found between the l.s. and h.s. forms, the imidazole nitrogen can adjust the structure accordingly. This in turn lowers the difference in bond order between the two forms for this Fe–N$^2$ bond. On the other hand, the pyridine, N$^1$, nitrogen is more rigid in its octahedral position (because of the relatively fixed imidazole rings) and therefore cannot move to a position of stronger bonding. The difference in the partial charge between the h.s. and l.s. forms on the iron (about 0.18) is about equally distributed among the co-ordinating nitrogens (about 0.04 for N$^1$ and about 0.03 for N$^2$).

As a measure of the donor strength of the substituents we used the $^1$H NMR increment (= $\Delta\delta$) for substituents X in the *para* position of benzene. The experimentally determined $\Delta\delta$ shows

**Table 8** Comparison of measured crystal structure of $[FeL_2][ClO_4]_2$ where X = H[27] with the calculated gas-phase structures where X = OH, Me, Cl, Br or H

| | Calculated (gas phase) | | | | | Measured (solid state) |
|---|---|---|---|---|---|---|
| Parameter[a] | X = OH | Me | Cl | Br | H | H |
| Fe–N(2) | 2.02 | 2.02 | 2.02 | 2.02 | 2.02 | 1.92 |
| Fe–N(22) | 2.14 | 2.14 | 2.14 | 2.12 | 2.13 | 1.94 |
| N(2)–Fe–N(22) | 79.0 | 79.0 | 79.0 | 78.5 | 79.0 | 79.60 |
| N(22)–Fe–N(24) | 157.9 | 157.9 | 157.9 | 157.0 | 158.0 | 160.80 |
| N(2)–Fe–N(2′) | 180[b] | 180[b] | 180[b] | 180[b] | 180[b] | 176.80 |
| N(2)–C(4)–C(18) | 110.7 | 110.6 | 110.7 | 110.6 | 110.6 | 109.70 |

[a] Bond lengths in Å, angles in °. For labelling see Scheme 2. [b] Assumed for these calculations.

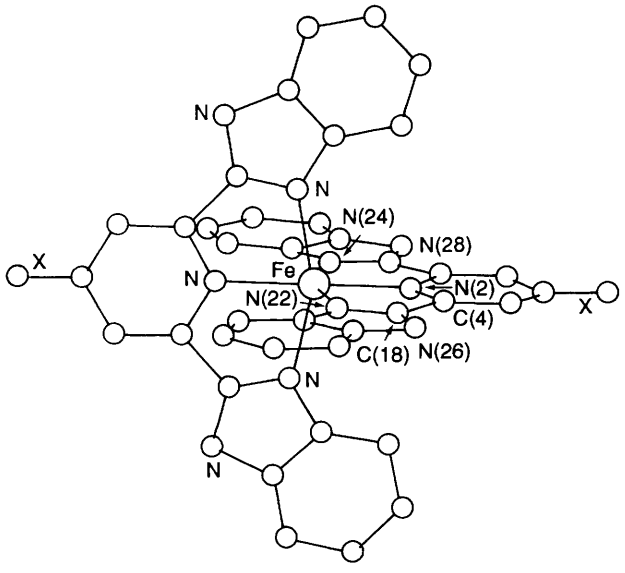


**Scheme 2** Structure of $[FeL_2]^{2+}$. Atoms pertinent to Table 8 only are labelled and refer to the respective atoms assigned in the second ligand

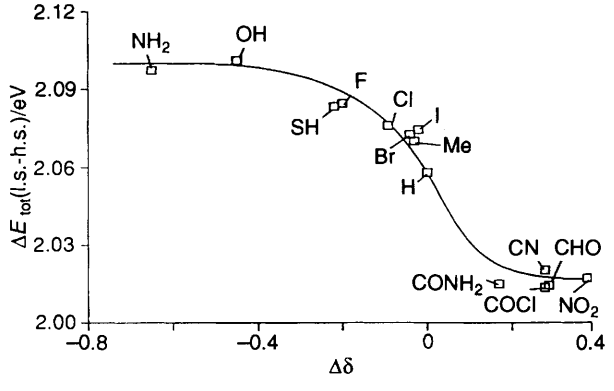


**Fig. 6** Differences in the calculated heats of formation between the h.s. and l.s. forms ($\Delta E_{tot}$ since calculations are for single molecules) in $[FeL_2]^{2+}$ *vs.* Δδ ($^1$H NMR increment for *para*-substituents X in benzene)

the sum of the influences from electron-withdrawing (−I) and electron-donating (+I) effects relative to the unsubstituted compound and therefore gives a measure of the mesomeric effect on the nitrogens $N^1$ and $N^2$. We found a good correlation between Δδ and the difference in the calculated heats of formation between the h.s. and l.s. forms (see Fig. 6). The curve shows a turning point at or near to the complex with X = H, so that a maximum sensitivity to substituent and environmental changes can be expected. Our calculations show that lower Δδ lead to lower electronic densities on the $N^1$ and to

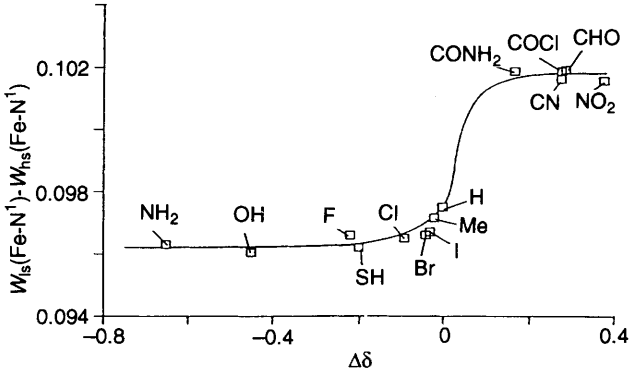


**Fig. 7** Difference in Wiberg indices for Fe–$N^1$ between the h.s. and l.s. forms of $[FeL_2]^{2+}$ *vs.* Δδ (see Fig. 6)

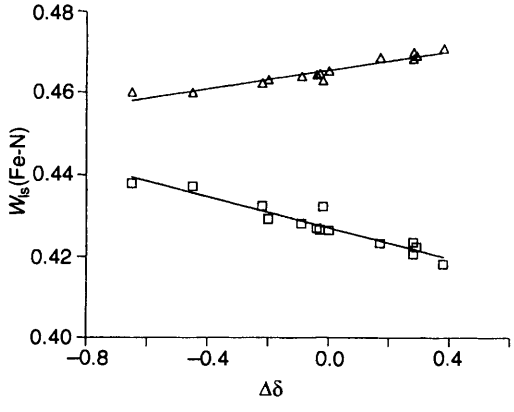


**Fig. 8** Wiberg indices for Fe–$N^1$ (□) and Fe–$N^2$ (△) in $[FeL_2]^{2+}$ *vs.* Δδ (see Fig. 6)

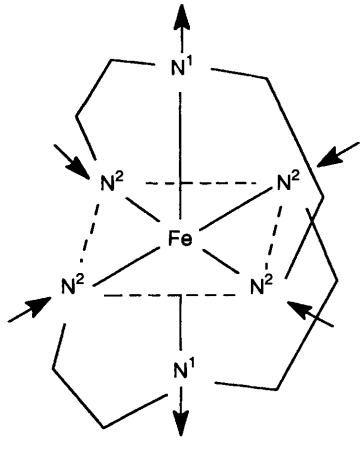


**Scheme 3** The modes of interaction of the nitrogens $N^2$ and $N^1$ with the iron

**Table 9** Bond orders (Wiberg indices) for Fe–$2N^1$ and Fe–$4N^2$ and partial charges for Fe, $N^1$ and $N^2$ and the difference in the heat of formation $\Delta H_{ls-hs}$ for the l.s. (spin multiplicity $m = 1$) and h.s. complexes ($m = 5$) resulting from QR-INDO calculations with different substituents X in $[FeL_2]^{2+}$

| Substituent X | Spin state | Bond order | | Charge/e | | | |
|---|---|---|---|---|---|---|---|
| | | Fe–$2N^1$ [a] | Fe–$4N^2$ [b] | Fe | $2N^1$ [a] | $4N^2$ [b] | $\Delta H_{ls-hs}$ [c]/eV |
| CHO | l.s. | 0.524 | 0.549 | −0.402 | 0.009 | −0.117 | 2.006 |
| | h.s. | 0.422 | 0.470 | −0.222 | −0.032 | −0.149 | |
| $NH_2$ | l.s. | 0.534 | 0.542 | −0.399 | −0.047 | −0.116 | 2.010 |
| | h.s. | 0.438 | 0.460 | −0.223 | −0.084 | −0.150 | |
| CN | l.s. | 0.525 | 0.548 | −0.401 | −0.001 | −0.116 | 2.012 |
| | h.s. | 0.423 | 0.468 | −0.223 | −0.034 | −0.151 | |
| H | l.s. | 0.524 | 0.549 | −0.401 | 0.004 | −0.117 | 2.053 |
| | h.s. | 0.427 | 0.465 | −0.223 | −0.034 | −0.151 | |
| Me | l.s. | 0.530 | 0.546 | −0.401 | −0.016 | −0.117 | 2.071 |
| | h.s. | 0.432 | 0.463 | −0.224 | −0.054 | −0.151 | |
| $NO_2$ | l.s. | 0.520 | 0.551 | −0.400 | 0.001 | −0.114 | 2.009 |
| | h.s. | 0.418 | 0.470 | −0.221 | −0.042 | −0.149 | |
| OH | l.s. | 0.533 | 0.542 | −0.398 | −0.056 | −0.115 | 2.100 |
| | h.s. | 0.437 | 0.460 | −0.222 | −0.093 | −0.149 | |
| $CONH_2$ | l.s. | 0.525 | 0.549 | −0.402 | 0.006 | −0.116 | 2.006 |
| | h.s. | 0.423 | 0.470 | −0.222 | −0.037 | −0.149 | |
| COCl | l.s. | 0.523 | 0.550 | −0.402 | 0.011 | −0.116 | 2.005 |
| | h.s. | 0.420 | 0.470 | −0.222 | −0.032 | −0.152 | |
| SH | l.s. | 0.529 | 0.545 | −0.399 | −0.029 | −0.116 | 2.080 |
| | h.s. | 0.433 | 0.462 | −0.222 | −0.067 | −0.150 | |
| F | l.s. | 0.526 | 0.546 | −0.397 | −0.038 | −0.114 | 2.082 |
| | h.s. | 0.429 | 0.463 | −0.220 | −0.075 | −0.149 | |
| Cl | l.s. | 0.525 | 0.547 | −0.398 | −0.024 | −0.115 | 2.072 |
| | h.s. | 0.428 | 0.464 | −0.221 | −0.061 | −0.149 | |
| Br | l.s. | 0.524 | 0.547 | −0.399 | −0.019 | −0.115 | 2.069 |
| | h.s. | 0.427 | 0.464 | −0.221 | −0.056 | −0.150 | |
| I | l.s. | 0.523 | 0.548 | −0.399 | −0.014 | −0.116 | 2.066 |
| | h.s. | 0.427 | 0.465 | −0.221 | −0.052 | −0.150 | |

[a] $2N^1$ = Averaged values of N-donor atoms of the two substituted pyridine rings. [b] $4N^2$ = Averaged values of N-donor atoms of the four substituted benzimidazole rings. [c] Difference in the heat of formation between the l.s. and h.s. forms.

higher electron densities on $N^2$. The same behaviour was found for the bond order of Fe–$N^1$ and Fe–$N^2$ (see Fig. 7). The turning point is again near to the unsubstituted species (X = H). This is in accord with the fact that the unsubstituted complex shows strong pronounced spin-crossover behaviour with temperature changes, whereas when X is OH or Cl there is only a low spin-crossover tendency. With increasing $\Delta\delta$, the bond order Fe–$N^1$ is reduced and that of Fe–$N^2$ increased (see Fig. 8). The binding forces for the equatorial imidazole $N^2$ atoms increase radially towards the iron centre while simultaneously the binding between the axial pyridine $N^1$ atoms and the iron decrease: this change in structure is illustrated in Scheme 3.

In conclusion, the pronounced spin-crossover behaviour found for $[FeL_2]^{2+}$ where X = H in solution is strongly reduced by electron-withdrawing substituents in the 4 position on the pyridine, leading eventually to pure high-spin states at room temperature in MeOH. This suggests, in accord with the ligand-field parameters evaluated from the nickel(II) complexes, that despite the strong electron-withdrawing properties of the substituents the ligand-field splitting in the substituted $[FeL_2]^{2+}$ species must be lower than that in the unsubstituted species, which is possibly due to a lowering of symmetry.[38]

## Acknowledgements

Thanks are due to the Fonds zur Förderung der wissenschaftlichen Forschung in Österreich for financial support under Projects 7605 and 8795. Professor R. F. Jameson (University of Dundee) is thanked for many useful discussions and for corrections to the manuscript.

## References

1 H. Toftlund, *Coord. Chem. Rev.*, 1989, **94**, 67.
2 K. Madeja and E. König, *J. Inorg. Nucl. Chem.*, 1963, **25**, 377.
3 L. Cambi and L. Szego, *Ber. Dtsch. Chem. Ges. B*, 1931, **64**, 259.
4 M. A. Hoselton, L. J. Wilson and R. S. Drago, *J. Am. Chem. Soc.*, 1975, **97**, 1722.
5 K. A. Reeder, E. V. Dose and L. Wilson, *Inorg. Chem.*, 1978, **17**, 1071.
6 M. G. Simmons and L. J. Wilson, *Inorg. Chem.*, 1977, **16**, 126.
7 A. W. Addison, S. Burman, C. G. Wahlgren, O. A. Rajan, T. M. Rowe and E. Sinn, *J. Chem. Soc., Dalton Trans.*, 1987, 2621.
8 J. P. Jesson, S. Trofimenko and D. R. Eaton, *J. Am. Chem. Soc.*, 1967, **89**, 3158.
9 D. M. L. Goodgame and A. A. S. C. Machado, *Inorg. Chem.*, 1969, **8**, 2031.
10 B. Strauss, W. Linert, V. Gutmann and R. F. Jameson, *Monatsh. Chem.*, 1992, **123**, 537.
11 B. Strauss, V. Gutmann and W. Linert, *Monatsh. Chem.*, 1992, **124**, 391, 515.
12 H. Li Chum, J. A. Vanin and M. I. D. Holanda, *Inorg. Chem.*, 1982, **21**, 1146.
13 R. F. Toomey and E. R. Riegel, *J. Org. Chem.*, 1952, **17**, 1492.
14 L. Haitinger and A. Lieben, *Monatsh. Chem.*, 1885, **6**, 285.
15 E. Königs and W. Jaschke, *Chem. Ber.*, 1921, **54**, 1351.
16 A. W. Addison and P. J. Burke, *J. Heterocycl. Chem.*, 1983, 1481.
17 D. F. Evans, *J. Chem. Soc.*, 1959, 2003.
18 D. S. Raiford, C. L. Fisk and E. D. Becker, *Anal. Chem.*, 1979, **51**, 2050.
19 R. F. Brunel and K. V. Bibber, *International Critical Tables*, McGraw-Hill, New York, London, 1930.
20 D. Ostfeld and I. A. Cohen, *J. Chem. Educ.*, 1972, **49**, 829.
21 R. Boca, Program MOSEM 7, Slovak Technical University, Bratislava, 1988.
22 R. Boca, *Int. J. Quantum Chem.*, 1987, **31**, 941.
23 R. Boca, *Int. J. Quantum Chem.*, 1990, **37**, 209.

24 R. Boca, *Int. J. Quantum Chem.*, 1988, **34**, 385.
25 R. Boca, *Czech. J. Phys.*, 1990, **B40**, 629.
26 R. Boca, *Int. J. Quantum Chem.*, 1988, **33**, 159.
27 S. Rüttimann, C. M. Moreau, A. F. Williams, G. Bernardinelli and A. W. Addison, *Polyhedron*, 1992, **11**, 635.
28 R. J. P. Williams, *J. Chem. Soc.*, 1955, 137.
29 C. K. Jørgensen, *Acta Chem. Scand.*, 1957, **11**, 166.
30 P. Krumholz, *Struct. Bonding (Berlin)*, 1971, **9**, 150.
31 P. Krumholz, *Inorg. Chem.*, 1965, **4**, 612.
32 W. J. Eillbeck and F. Holmes, *J. Chem. Soc. A*, 1967, 1777.
33 H. Irving and D. P. Mellor, *J. Chem. Soc.*, 1962, 5222.
34 A. J. Pople, W. G. Schneider and H. J. Bernstein, *High Resolution Nuclear Magnetic Resonance*, McGraw-Hill, New York, 1959.
35 R. C. West (Editor), *CRC Handbook of Chemistry and Physics*, 67th edn., CRC Press, Boca Raton, FL, 1986.
36 T. Hahn (Editor), *International Tables for Crystallography*, International Union of Crystallography, Reidel, Dordrecht, 1983, vol. A.
37 E. Pretsch, T. Clerk, J. Seibl and W. Simon, *Tabellen zur Strukturaufklärung organischer Verbindungen mit spektroskopischen Methoden*, Springer, Berlin, Heidelberg, New York, 1990.
38 L. Wang, Y. Zhu, F. Fangjie, Q. Wang and L. Wang, *Polyhedron*, 1992, **11**, 1909.

*Received* 20*th December* 1993; *Paper* 3/07448J